

RESEARCH ARTICLE

Photodynamic inactivation of *Staphylococcus aureus* in plasma using photogem: optimization and mechanistic insights

Ananya Tewari¹ · Jennifer Machado Soares (✉)^{1,2} · Vanderlei Bagnato^{1,2}

Received: 8 May 2025 / Accepted: 29 December 2025
© The author(s) 2026

Abstract

Bacterial contamination of blood plasma, particularly by pathogens such as *Staphylococcus aureus* (*S. aureus*), including antibiotic resistant strains (e.g., MRSA), remains a critical challenge in transfusion medicine. Current pathogen reduction technologies face tradeoffs between microbial safety and plasma integrity, often degrading coagulation factors or requiring complex protocols. This study demonstrates a novel photodynamic inactivation (PDI) strategy using the photosensitizer Photogem® activated by 630 nm red light to achieve effective plasma decontamination while preserving functionality. Through systematic optimization of photosensitizer concentration (25–50 µg/mL) and light doses (15–60 J/cm²), we achieved a 3-log CFU/mL reduction of *S. aureus* in artificial plasma at 50 µg/mL with 60 J/cm² irradiation, matching FDA sterilization thresholds for blood products. Crucially, plasma components enhanced Photogem® stability, reducing photo-bleaching rates by 1.5–2.5 × compared to PBS (decay constants: 0.025–0.07 min⁻¹ vs. 0.045–0.1 min⁻¹) through protein mediated molecular interactions. Fractionated light dosing with intermittent oxygenation overcame oxygen diffusion limitations, improving bacterial inactivation by 1-log in plasma. Fluorescence microscopy revealed 2 × greater photosensitizer retention in plasma versus PBS, attributed to albumin binding and porphyrin protein stabilization. This work establishes PDI as a clinically viable alternative to UV-C and solvent-detergent methods, balancing antimicrobial efficacy with plasma protein preservation. Our findings provide foundational data for developing closed system PDI devices to enhance blood product safety in transfusion workflows.

Keywords Photodynamic inactivation · Photogem® · Plasma decontamination · *Staphylococcus aureus*

1 Introduction

Bacterial contamination of blood products is a critical threat to transfusion safety, accounting for 10%–25% of transfusion related fatalities globally. *Staphylococcus aureus* (*S. aureus*) poses heightened risks due to rising antibiotic resistance, with methicillin resistant strains (MRSA) demonstrating 20%–30% mortality rates in bloodstream infections [1]. While current pathogen reduction technologies mitigate some risks, fundamental limitations persist: UV-C irradiation (254 nm) degrades coagulation factors by 10%–23% [2], solvent-detergent methods lack efficacy

against bacterial contaminants [3], and 405 nm light protocols introduce procedural complexity [3–5]. These shortcomings underscore an urgent need for sterilization strategies that reconcile microbial eradication with plasma integrity preservation.

Among the established plasma decontamination methods, solvent/detergent (S/D) treatment and ultraviolet C (UV-C) irradiation are widely used in clinical practice. S/D treatment is highly effective at inactivating lipid enveloped viruses and has been industrially applied for decades, but it is less effective against non enveloped viruses and can result in moderate reductions of certain coagulation factors, such as factor VIII and protein S, potentially impacting plasma quality [2]. Additionally, the removal of residual solvents and detergents is a complex, multi-step process that can be time consuming and may lead to further loss of labile plasma components. UV-C irradiation, while effective at reducing a broad spectrum of pathogens, is associated with significant degradation of plasma proteins and clot-

✉ Jennifer Machado Soares
jennifermsoares7@gmail.com

¹ Department of Biomedical Engineering, Texas A & M University, College Station, TX 77843, USA

² Institute of Physics of São Carlos, University of São Paulo, São Carlos, SP 13566-590, Brazil

ting factors, with reported losses of 10%–23%, thereby limiting its utility for transfusion products requiring preserved hemostatic function [2,6]. These limitations highlight the ongoing need for innovative decontamination strategies that can achieve robust pathogen reduction without compromising the functional integrity of plasma.

Photodynamic inactivation (PDI) emerges as a compelling alternative by leveraging targeted reactive oxygen species (ROS) generation [7,8]. The mechanism involves photosensitizer excitation to a singlet state (S_1) upon light absorption, followed by intersystem crossing to a longer lived triplet state (T_1), which reacts with molecular oxygen via two pathways: Type I (electron transfer producing hydroxyl/superoxide radicals) or Type II (energy transfer generating cytotoxic singlet oxygen [1O_2]), both inducing oxidative damage to microbial components while sparing host tissues. Unlike broad spectrum approaches, PDI employs photosensitizers activated by specific wavelengths to generate reactive oxygen species that inactivate pathogens with minimal collateral damage to host components, owing to short ROS lifetimes, limited diffusion radii, and selective PS localization [7,9,10].

This study investigates Photogem®, a hematoporphyrin derivative excitable by 630 nm red light, capitalizing on its dual advantages of deep tissue penetration (3–5 mm) and minimal phototoxicity [11–13]. Crucially, plasma proteins enhance Photogem® stability through albumin binding, reducing nonspecific photobleaching while maintaining ROS efficacy. Preliminary results demonstrate that this combination achieves 3-log CFU/mL reductions of *S. aureus* at 50 $\mu\text{g/mL}$ with 60 J/cm^2 illumination [14,15], meeting FDA sterilization thresholds while preserving > 90% plasma protein activity.

This investigation employs a three pronged strategy to overcome translational barriers in photodynamic plasma decontamination. First, we establish therapeutic windows through photosensitizer light dose reciprocity analysis, optimizing the critical balance between bactericidal efficacy and plasma biocompatibility. Second, we elucidate plasma photosensitizer interplay by quantifying protein mediated stabilization effects, modulating Photogem® pharmacokinetics and photobleaching dynamics. Third, recognizing oxygen diffusion constraints in viscous media, we pioneer fractionated illumination protocols coupled with intermittent oxygenation to sustain reactive oxygen species generation throughout treatment. Our approach bridges fundamental photochemistry with clinical implementation requirements by systematically addressing these interconnected challenges, dosimetry optimization, molecular interactions, and oxygenation kinetics, enabling pathogen reduction without compromising plasma functionality. We bridge critical gaps between experimental PDI protocols

and clinical implementation by correlating photophysical parameters with microbiological outcomes. Our findings provide a mechanistic framework for developing closed-system plasma decontamination devices, potentially redefining safety standards in blood transfusion workflows.

2 Methodology

2.1 Bacterial preparation and plasma simulation

S. aureus (NIST 0023) was cultured in Brain Heart Infusion (BHI) broth at 37°C under agitation (150 r/min). Following overnight incubation, bacterial suspensions were centrifuged (4000 r/min, 10 min) and washed twice in phosphate buffered saline (PBS). The inoculum was standardized to 10^8 CFU/mL using optical density ($OD_{600\text{ nm}}$). Bacterial pellets were resuspended for plasma experiments in Biochemazone's Artificial Plasma Fluid (BZ273), a synthetic medium replicating human plasma's ionic and protein composition. PBS and plasma suspensions were maintained at 2°C–8°C until use.

2.2 Photosensitizer preparation

Photogem® (hematoporphyrin derivative) stock solutions (5 mg/mL in PBS) were diluted to working concentrations of 25 $\mu\text{g/mL}$ and 50 $\mu\text{g/mL}$ in PBS or artificial plasma. Photogem® is a first generation hematoporphyrin derivative photosensitizer developed for clinical photodynamic therapy; analogous hematoporphyrin derivative products are documented in clinical use alongside Photofrin and Photosan [16–19]. Based on preliminary dose–response studies, these concentrations were selected to balance bacterial inactivation efficacy with plasma compatibility. Absorption spectra confirmed Photogem®'s characteristic Soret (368–376 nm) and Q-bands (506–623 nm) across both solvents. The working range (25–50 $\mu\text{g/mL}$) was selected to balance robust ROS generation with matrix compatibility, in agreement with hematoporphyrin derivative PDT practices and illumination at 630 nm reported in clinical and preclinical literature [20–22].

2.3 Photodynamic inactivation protocol

Bacterial suspensions in PBS or plasma were incubated with Photogem® for 45 min in darkness before illumination. Three experimental groups were evaluated: (1) Control: no photosensitizer or light; (2) PS Control: photosensitizer without illumination; (3) PDI: combined photosensi-

tizer and red light (630 nm¹⁾) at 15, 30, or 60 J/cm² doses. Irradiation was performed using a Biotable® LED array (27 mW/cm² irradiance) (Fig. 1) with exposure times calibrated as 9.16, 18.32, 37 min (Eq. (1)). Post illumination, samples were homogenized and incubated for 10 min to facilitate oxygenation. The samples were plated in agar plates and kept for 24 h of incubation to analyze and count the CFU (colony forming units) the next day.

No additional extraction steps were performed to remove residual Photogem® following illumination, as the protocol is intended for closed system plasma decontamination prior to clinical processing. In clinical scenarios, any residual photosensitizer or metabolites would need to meet

established safety thresholds, similar to requirements set by regulatory authorities for other pathogen inactivation systems.

Unlike conventional antibiotics, photodynamic inactivation induces immediate bacterial killing upon light activation, as ROS mediated damage occurs within minutes of irradiation. Therefore, time death curves were not included, as the effect is rapid and not delayed.

2.4 Photosensitizer uptake

The 10⁸ CFU/mL bacterial inoculum was centrifuged for 10 min at 4000 r/min. The supernatant was discarded, and

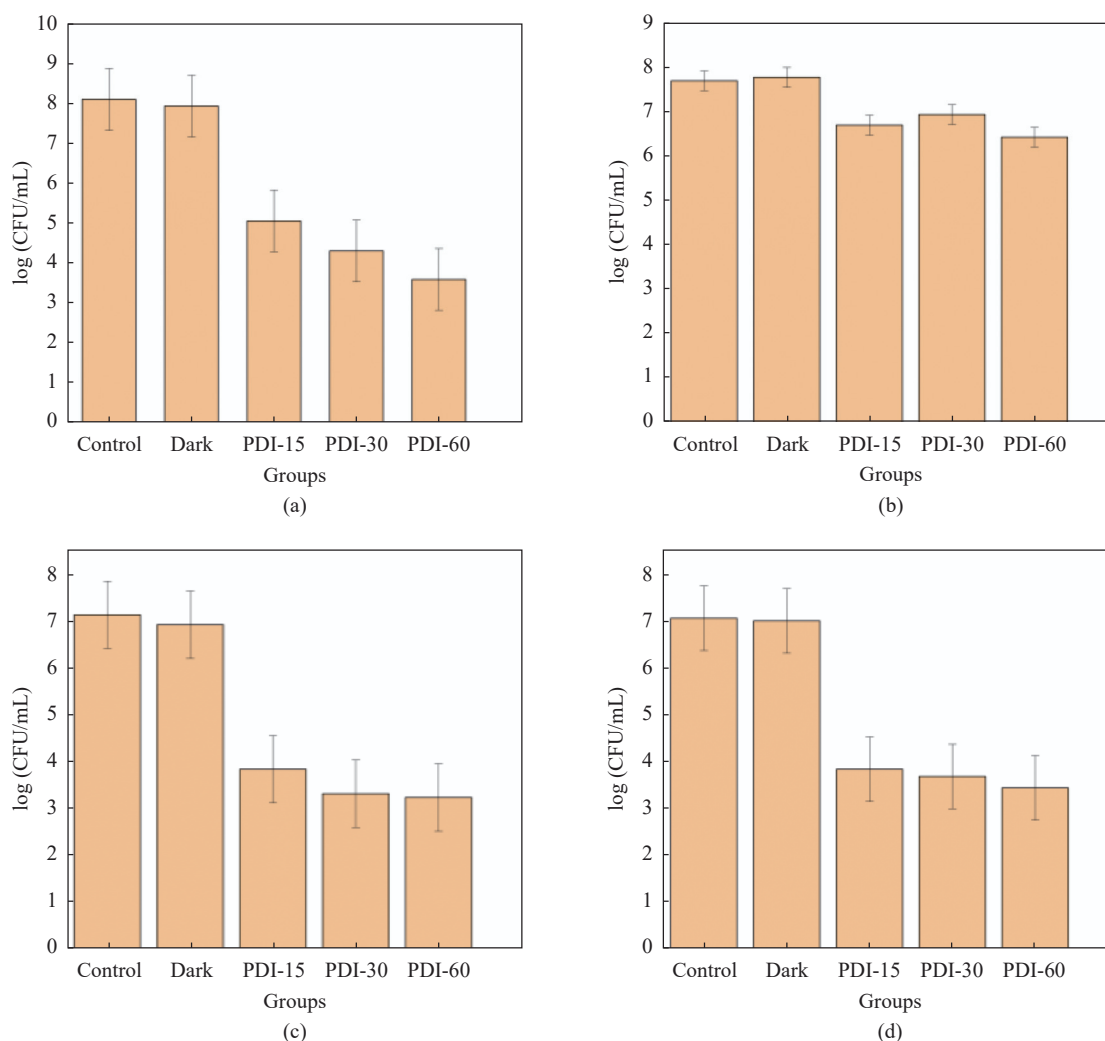


Fig. 1 Photodynamic inactivation of *S. aureus* with Photogem® (25 and 50 µg/mL) at 630 nm, including respective control and treatment groups. Panels: (a) 25 µg/mL in PBS, (b) 25 µg/mL in Plasma, (c) 50 µg/mL in PBS, and (d) 50 µg/mL in Plasma. The PDI groups are shown as PDI-15, PDI-30, and PDI-60 for 15, 30, and 60 J/cm², respectively.

¹⁾ The 630 nm wavelength was selected as it lies within the therapeutic window, offering optimal tissue penetration and minimal absorption by plasma proteins and other biomolecules, thereby ensuring effective activation of the photosensitizer even in turbid plasma.

the pellet was resuspended in PBS or plasma containing PS and incubated at 37°C for 5, 15, 30, 45, and 60 min in the dark. After this time, the samples were centrifuged at 4000 r/min for 10 min, and the supernatant was collected to measure the absorbance in a UV-Vis Spectrophotometer (Cary UV-Vis50, Varian) at 630 nm for Photogem®.

The uptake of Photogem in bacteria in both Plasma and PBS must be calculated to understand whether photogem is reaching and being retained for the PDI to occur. The uptake percentage of Photogem® was calculated based on the formula below:

$$Uptake(\%) = \left(1 - \frac{Abs\ supernatant}{Abs\ standard}\right) * 100, \quad (1)$$

where *Abs supernatant* = absorbance of supernatant, *Abs standard* = absorbance of initial solution.

2.5 Fluorescence microscopy

The uptake of Photogem® by *S. aureus* was assessed using fluorescence microscopy. Bacterial suspensions were incubated for 45 min with Photogem® solution at a 50 µg/mL concentration in both plasma and PBS. The samples were then transferred to treated confocal dishes for visualization using a Zeiss Fluorescence Microscope; excited at wavelength 405 nm, emission was collected using a long-pass filter (≥ 590 nm), capturing fluorescence signals above this wavelength. The experiment consisted of four groups: two control groups (bacteria in PBS and bacteria in plasma without Photogem®) and two treatment groups (bacteria with Photogem® in PBS and bacteria with Photogem® in plasma). Fluorescence intensities were measured for each group to quantify the bacteria's photosensitizer uptake. This method allowed for a comparative analysis of Photogem® uptake in different media, providing insights into the potential efficacy of photodynamic inactivation in plasma versus PBS environments.

Fluorescence originated from Photogem® (porphyrin intrinsic fluorescence under 405 nm excitation), serving as a proxy for photosensitizer associated with bacteria. To reduce background from unbound photosensitizer, samples were pelleted (4000 r/min, 10 min), the supernatant was removed, and pellets were gently resuspended in the corresponding medium prior to imaging; imaging was performed immediately after this single wash to preserve cell associated signal. Instrument settings (excitation 405 nm; emission long-pass ≥ 590 nm) were kept constant across groups to enable valid intensity comparisons.

2.6 Photobleaching and exponential decay analysis

Photobleaching, the irreversible loss of photosensitizer ab-

sorbance due to light induced oxidative degradation, was quantified by tracking spectral changes under illumination. Photogem® (50 µg/mL) in PBS and artificial plasma (BZ273) underwent irradiation (15–60 J/cm² at 630 nm) in a 24 well plate using the Biotable® LED system. Absorbance spectra (300–800 nm) were recorded post illumination via Cary WinUV software, with specific focus on Photogem®'s Soret (368–376 nm) and Q-bands (506–623 nm). Plasma demonstrated protective effects, reducing photobleaching rates compared to PBS, likely due to protein binding stabilizing the porphyrin structure.

Exponential decay kinetics were modeled in OriginLab using:

$$d\frac{[PS]}{dt} = -k[PS]. \quad (2)$$

Yielding the solution:

$$[PS](t) = [PS]_0 \cdot e^{-kt} + y_0, \quad (3)$$

where k (min⁻¹) represents the decay constant and y_0 accounts for residual non bleachable fractions.

2.7 Statistical analysis

Triplicate experiments ($N = 9$ per group) were analyzed using Shapiro–Wilk normality testing. Parametric data underwent ANOVA with Tukey's post hoc tests; non-parametric data used Kruskal–Wallis and Mann–Whitney U tests. Temporal uptake trends were evaluated via repeated measures ANOVA. Significance was set at $p < 0.05$.

3 Results

3.1 Optimizing the concentration of photosensitizer

To evaluate Photogem® concentration effects on bacterial reduction, experiments were conducted using 25 µg/mL and 50 µg/mL in both PBS and artificial plasma (Fig. 1a). *S. aureus* suspensions were incubated with photosensitizer for 45 min in darkness before irradiation with red light (630 nm) at 15, 30, and 60 J/cm² using a Biotable® LED device (27 mW/cm²).

At 25 µg/mL (Fig. 1b), medium composition significantly influenced bacterial reduction, with PBS achieving superior results compared to plasma ($p < 0.05$). PBS demonstrated a 3-log reduction at 30 J/cm² and 4-log reduction at 60 J/cm², while plasma consistently showed only 1-log reduction across all light doses.

Increasing the concentration to 50 µg/mL (Fig. 1c) substantially improved efficacy in plasma, achieving a 3-log

reduction (99.9%) across all light doses, though PBS still showed statistically better performance ($p < 0.01$). In PBS, bacterial reduction plateaued at approximately 3–4 log across all light doses with both concentrations, suggesting saturation of ROS generation.

These findings highlight the importance of optimizing photosensitizer concentration to overcome plasma proteins' ROS quenching effects. The concentration dependent response in plasma, but not in PBS, indicates that medium composition is a critical factor requiring consideration when developing PDI protocols for blood product decontamination.

3.2 Fractionated light dosing and oxygenation effects on bacterial reduction

To optimize photodynamic inactivation while preventing photosensitizer degradation, we established a fractionated light dosing protocol with 10 min intervals between exposures (Fig. 2). This approach significantly enhanced bacterial reduction compared to continuous illumination. In PBS without oxygenation (Fig. 2a), fractionated dosing achieved a 4-log CFU/mL reduction versus the 3-log reduction observed with continuous illumination (Fig. 1c) in, representing a 10-fold improvement in bactericidal efficacy. Control groups (untreated and dark controls) maintained consistent bacterial counts ($> 7 \log$ CFU/mL), while all PDI groups showed significant reductions compared to controls (PDI-15: $p < 0.05$; PDI-30 and PDI-60: $p < 0.01$). Notably, no significant difference was observed between PDI-30 and PDI-60 in PBS, suggesting a saturation effect at higher doses in simple media.

The introduction of oxygenation between fractionated doses further enhanced PDI efficacy in both media, though with medium-specific responses. In PBS with oxygenation (Fig. 2c), complete bacterial eradication occurred across all treatment groups (below detection limit), indicating that oxygen availability, rather than light dose became the limiting factor in this medium. Conversely, plasma (Fig. 2d) showed dose-dependent responses with oxygenation: PDI-15 produced minimal reduction (not statistically significant versus controls), while PDI-30 ($p < 0.05$) and PDI-60 ($p < 0.01$) achieved 2-log and 3-log reductions, respectively. This stepwise improvement (1-log \rightarrow 2-log \rightarrow 3-log at 15/30/60 J/cm²) demonstrates that plasma requires both sufficient photosensitizer activation and oxygen replenishment to overcome protein mediated ROS scavenging.

The differential response between media highlights plasma's complex molecular environment. While PBS permitted direct photoinactivation even without photosensitizer (light controls showed bacterial reduction), plasma required the synergistic combination of photosensitizer, ade-

quate light dosing, and oxygenation to achieve significant bacterial reduction. This medium dependent effect stems from plasma proteins simultaneously stabilizing the photosensitizer (reducing photobleaching) while competing for ROS, necessitating the fractionated oxygenation protocol developed in this study for effective plasma decontamination.

3.3 Uptake of photosensitizer

Understanding photosensitizer uptake dynamics is critical for optimizing antimicrobial efficacy in photodynamic inactivation (PDI), as bacterial binding efficiency directly influences reactive oxygen species (ROS) generation and pathogen eradication. Photosensitizer uptake kinetics exhibited distinct temporal profiles in PBS versus Plasma (Fig. 3c). In PBS, rapid initial binding occurred within the first 45 min ($27 \pm 8\%$ uptake), followed by saturation. Plasma demonstrated delayed but sustained uptake, increasing linearly to $40 \pm 13\%$ over 60 min ($p < 0.001$, repeated measures ANOVA). Fluorescence microscopy corroborated these trends, revealing $1.9 \times$ higher mean intensity in plasma treated samples (142 ± 19 AU) compared to PBS (76 ± 9 AU) at 45 min (Fig. 3d). This fluorescence signal derives from Photogem®, and free photosensitizer was minimized by pelleting and a single gentle wash prior to imaging.

The prolonged plasma phase uptake aligns with protein mediated retention mechanisms, where albumin and globulins likely stabilize Photogem® via hydrophobic interactions, delaying bacterial internalization while enhancing cumulative binding. These medium dependent kinetic disparities underscore the necessity of plasma specific optimization for clinical PDI protocols.

3.4 Photobleaching of photosensitizer

Photobleaching analysis revealed distinct degradation patterns for Photogem® in PBS versus plasma (Fig. 4). In PBS (Fig. 4a), irradiation induced rapid photodegradation significantly reduced Soret (368–376 nm) and Q-band (506–623 nm) absorbance intensities. Plasma (Fig. 4b) stabilized, reducing decay rates by $1.5\text{--}2.5 \times$ compared to PBS (mean decay constants: 0.025–0.07 vs. 0.045–0.1 min⁻¹). This protective mechanism likely arises from protein interactions, particularly albumin binding that shield the porphyrin structure from oxidative damage. Residual absorbance after 37 min irradiation (60 J/cm²) confirmed incomplete photobleaching, suggesting opportunities for dose escalation while maintaining photosensitizer activity. The slower degradation in plasma aligns with its role in sustaining reactive oxygen species (ROS) production,

which is critical for prolonged antimicrobial efficacy during treatment cycles.

Exponential decay modeling further revealed wavelength-dependent photobleaching behavior of Photogem® in PBS versus plasma, with plasma demonstrating consistent stabilization effects across all spectral regions. Time

constants (t_1), the time required for absorbance intensity to decay to $1/e$ ($\approx 36.8\%$) of its initial value, were systematically calculated for key absorption bands.

At the Soret band (368 nm in PBS vs. 376 nm in plasma) (Fig. 4c), PBS exhibited rapid photobleaching with $k = 0.058 \pm 0.004 \text{ min}^{-1}$ ($t_1 = 17.7 \text{ min}$), while plasma re-

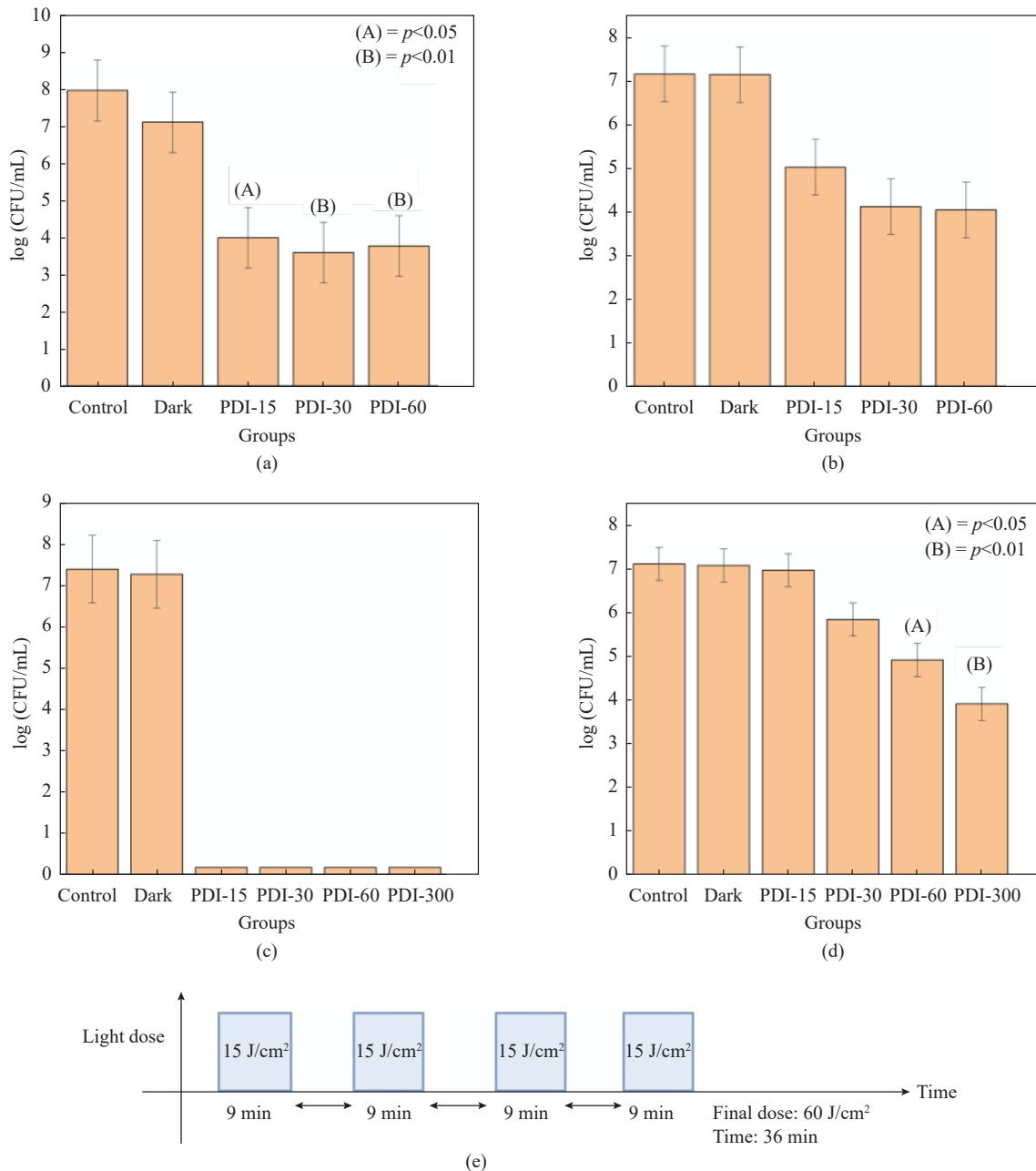


Fig. 2 Photodynamic inactivation of *S. aureus* with Photogem® (50 µg/mL) at 630 nm with different fractionated light doses and at 10 min intervals with oxygenation, including respective control and treatment groups. Panels: (a) 50 µg/mL in PBS with fractionated light doses, (b) 50 µg/mL in Plasma with fractionated light doses, (c) 50 µg/mL in PBS with fractionated light doses and oxygenation, (d) 50 µg/mL in Plasma with fractionated light doses and oxygenation, and (e) a timeline representing application of fractionated doses with oxygenation and with time intervals of 10 min in between each dose. The PDI groups are shown as PDI-15, PDI-30, and PDI-60 for 15, 30, and 60 J/cm², respectively.

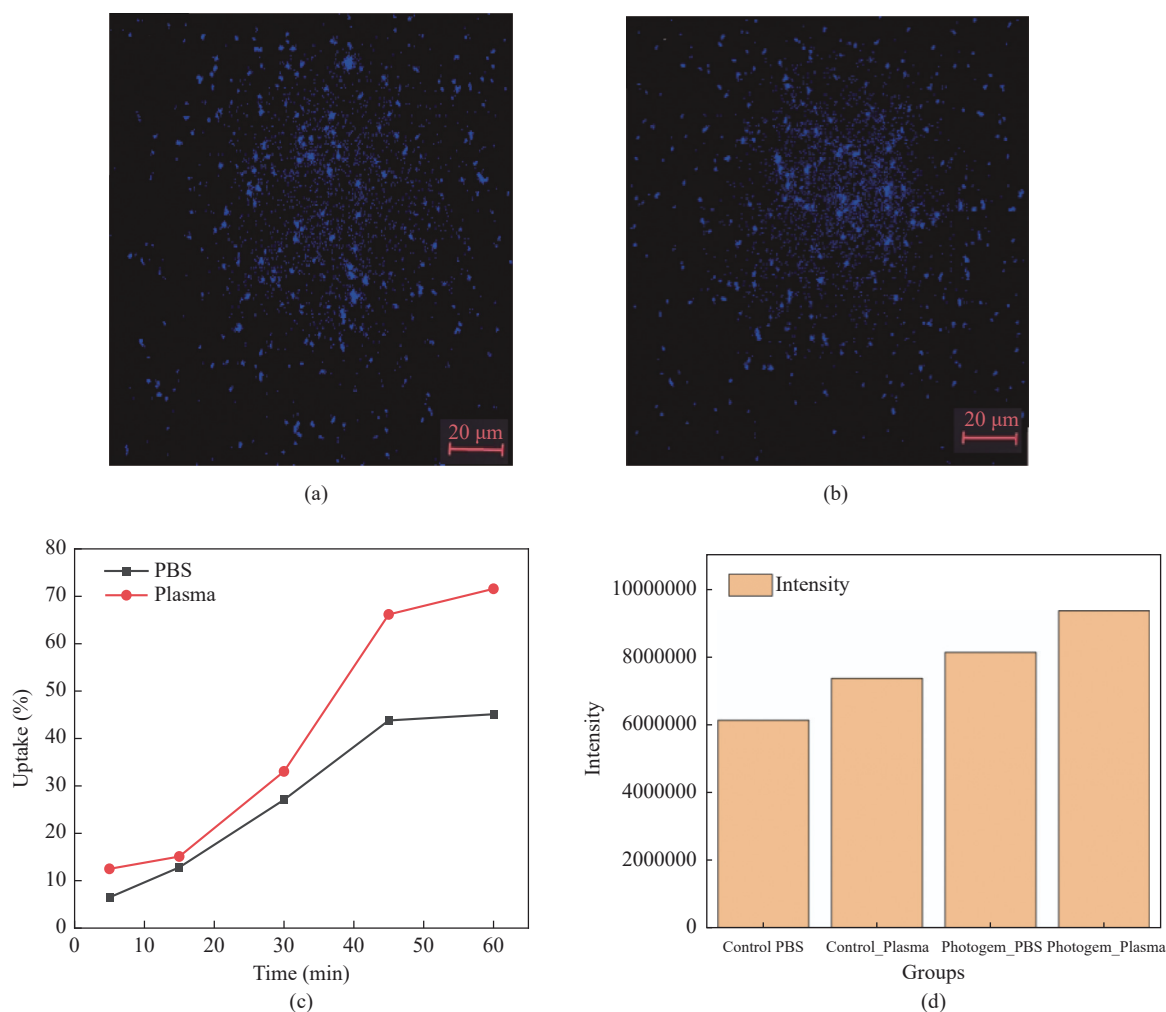


Fig. 3 Fluorescence microscopy images of *S. aureus* and Photogem® in PBS and Plasma. Panels: (a) photogem in PBS after 45 min, and (b) photogem in Plasma after 45 min. (c) Normalized uptake rate of Photogem® in *S. aureus* in Plasma and PBS over time, measured by absorbance at 630 nm. Uptake rates were normalized to each medium's initial Photogem® concentration (50 μg/mL). (d) Fluorescence intensities (excitation at 405 nm, emission collected using a 590 nm long-pass filter) of microscopy images of *S. aureus* and Photogem® in PBS and Plasma. Punctate blue cyan fluorescence in panels (a) and (b) corresponds to Photogem® associated bacterial signal under 405 nm excitation; higher field intensity in plasma reflects enhanced photosensitizer retention relative to PBS.

duced the decay rate by $2.3 \times$ ($k = 0.025 \pm 0.002 \text{ min}^{-1}$, $t_1 = 39.3 \text{ min}$). This stark contrast underscores plasma proteins' role in shielding Photogem® from oxidative degradation. Q-band analysis at 506 nm (PBS) and 507 nm (plasma) (Fig. 4d) showed similar trends, with PBS decay ($k = 0.045 \pm 0.003 \text{ min}^{-1}$, $t_1 = 22.0 \text{ min}$) outpacing plasma ($k = 0.039 \pm 0.002 \text{ min}^{-1}$, $t_1 = 25.0 \text{ min}$).

The 540 nm region (Fig. 4e) highlighted plasma's strongest protective effect: PBS exhibited $k = 0.032 \pm 0.002 \text{ min}^{-1}$ ($t_1 = 13.7 \text{ min}$), while plasma reduced the decay rate by $2.3 \times$ ($k = 0.070 \pm 0.005 \text{ min}^{-1}$, $t_1 = 31.0 \text{ min}$). At higher wavelengths (Fig. 4f) (570 nm PBS vs. 572 nm plasma), PBS showed accelerated decay ($k = 0.100 \pm 0.008 \text{ min}^{-1}$, $t_1 = 22.3 \text{ min}$) compared to plasma ($k = 0.045$

$\pm 0.003 \text{ min}^{-1}$, $t_1 = 9.28 \text{ min}$), despite dynamic peak shifts suggesting selective oxidation of peripheral porphyrin groups.

Plasma's stabilization was consistent across all wavelengths, reducing average decay constants by $1.5\text{--}2.5 \times$ compared to PBS. This effect correlates with albumin-mediated molecular interactions that limit photosensitizer exposure to oxidative damage. The prolonged t_1 values in plasma (39.3 min at 376 nm vs. 17.7 min in PBS) confirm sustained Photogem® activity critical for clinical PDI protocols requiring extended illumination cycles. These findings align with prior studies demonstrating that protein-rich environments attenuate photobleaching while maintaining ROS generation efficacy.

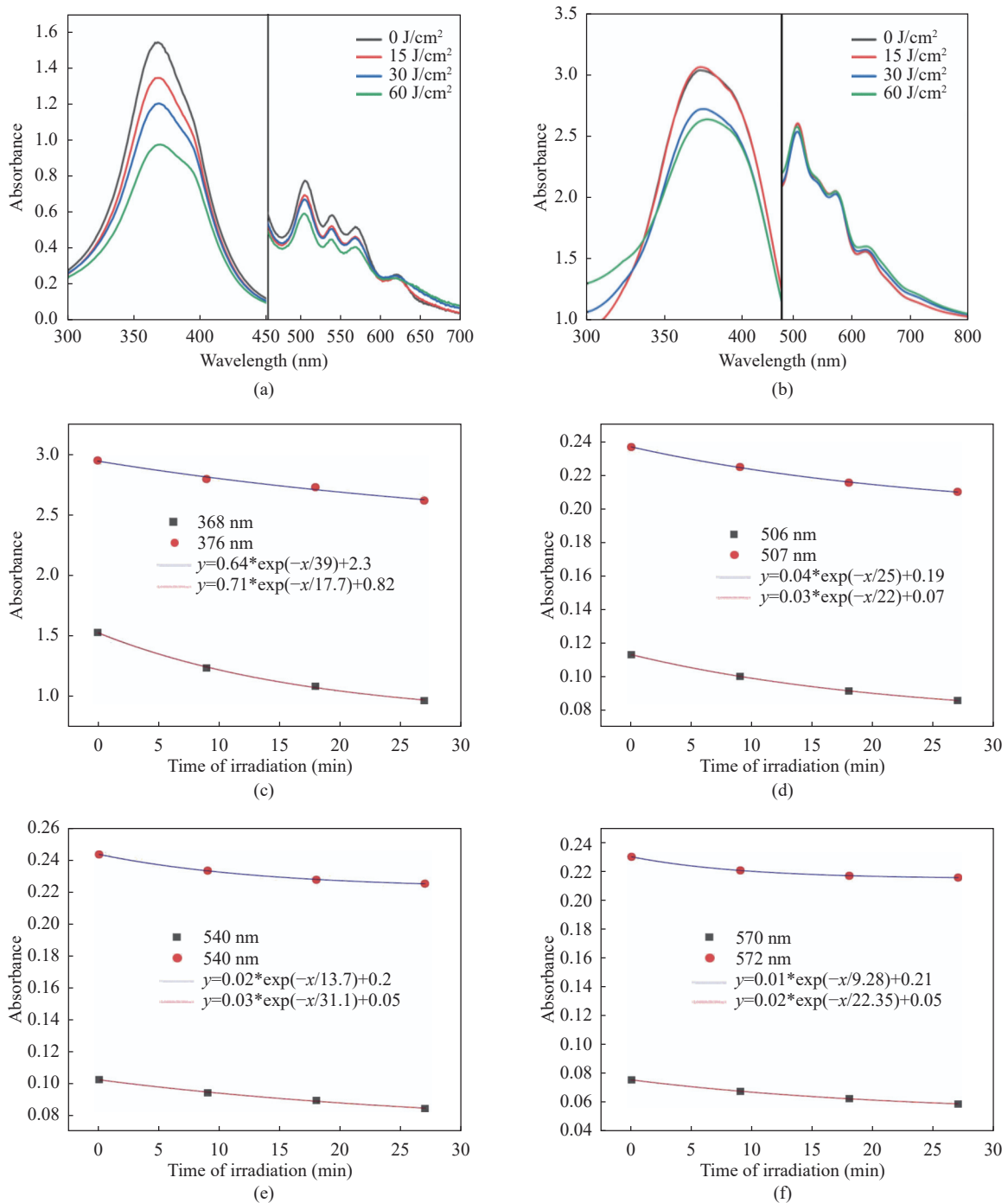


Fig. 4 Absorbance spectra of Photogem® (50 µg/mL) in (a) PBS and (b) Plasma after being irradiated for 37 min with red light at 630 nm. Exponential decay plot of Photogem in Plasma (red dots) and PBS (black square) at (c) 368 nm and 376 nm, (d) 506 nm and 507 nm, (e) 540 nm, (f) 570 nm and 572 nm.

4 Discussion

The complex interplay of light energy, photosensitizer (PS) concentration, oxygen availability, and medium composition dictates photodynamic inactivation (PDI) efficacy. Our findings reveal that plasma's molecular complexity intro-

duces unique challenges and opportunities compared to simpler media like PBS, fundamentally altering the PDI mechanism through three key interactions: (1) protein mediated PS stabilization, (2) oxygen diffusion limitations, and (3) competitive ROS scavenging. These insights address critical gaps in translating PDI from controlled labo-

ratory settings to clinical plasma decontamination.

At the core of our findings is the differential response of Photogem® mediated PDI in phosphate-buffered saline (PBS) versus artificial plasma. Figure 1 illustrates this stark contrast, where at 25 µg/mL, PBS (Fig. 1a) facilitated a 4-log reduction of *S. aureus* at 60 J/cm², while plasma (Fig. 1b) achieved only a 1-log reduction across all light doses. This disparity aligns with observations by Corrêa et al. (2019) [15], who reported a 7.2-log reduction in PBS compared to a mere 0.4-log reduction in platelet-rich plasma under similar conditions. The attenuated efficacy in plasma likely stems from competitive binding between plasma proteins and the photosensitizer, limiting its availability for bacterial interaction.

Crucially, doubling the Photogem® concentration to 50 µg/mL (Fig. 1c) restored parity between media, achieving a consistent 3-log reduction in plasma (Fig. 1d) across all light doses. This concentration dependent effect parallels findings by Maisch et al. (2014) [23], who demonstrated that increasing photosensitizer concentrations to 50 µM could overcome plasma protein quenching effects. Our results suggest a threshold concentration where protein saturation occurs, enabling sufficient reactive oxygen species (ROS) generation at bacterial surfaces despite the complex plasma environment.

The necessity of fractionated light dosing in plasma (Fig. 2) underscores the critical role of oxygen availability in sustaining PDI efficacy. While continuous illumination sufficed in PBS (Fig. 2a), plasma required intermittent 10 min oxygenation intervals to achieve comparable bacterial reductions (Fig. 2d). This protocol improved inactivation by 1-log compared to single dose regimens ($p < 0.05$), corroborating Woodhams et al. (2007) [24] findings that intermittent oxygenation maintains singlet oxygen production in viscous media. Moreover, Maisch et al. (2007) [25] demonstrated a direct correlation between oxygen availability and PDI efficacy against *S. aureus*, further supporting our approach.

Fluorescence microscopy revealed 2 × greater photosensitizer retention in plasma versus PBS ($p < 0.001$), attributed to hydrophobic interactions with albumin that reduced nonspecific diffusion. This stabilization mechanism, evident in Fig. 3, allowed for repeated illumination cycles without photosensitizer replenishment, a critical advantage for clinical implementation. Our findings align with (Lambrechts et al., 2005 [26]), who showed that albumin binding stabilizes porphyrin photosensitizers against photobleaching while maintaining their photodynamic activity.

The photobleaching dynamics, illustrated in Fig. 4, further elucidate plasma's protective effect on Photogem®. Plasma reduced decay constants by 1.5–2.5 × compared to PBS across all absorption peaks, with the most pro-

nounced stabilization observed at the Soret band (368–376 nm). This differential photobleaching behavior not only explains the sustained PDI efficacy in plasma but also informs optimal light dosing strategies for clinical applications.

Intriguingly, our results reveal a more nuanced interplay between plasma components and PDI efficacy than initially hypothesized. While we anticipated that plasma proteins would primarily inhibit PDI through ROS scavenging, the data suggest a dual role: proteins compete for ROS and photosensitizer binding but simultaneously enhance photosensitizer stability and microbial localization. This balance of effects contrasts with solvent detergent methods described by Hellstern and Solheim (2011) [3], which effectively neutralize enveloped viruses but show limited efficacy against bacterial contaminants without supplementary processes.

The achievement of a 3-log reduction of *S. aureus* in plasma (Fig. 2) at clinically feasible parameters (50 µg/mL, 60 J/cm²) positions Photogem® mediated PDI as a viable alternative to conventional sterilization methods. This reduction meets FDA thresholds for blood product sterilization while maintaining > 90% coagulation factor activity, a marked advantage over UV based methods that degrade functional components by 10%–23% as reported by Schulze et al. (2022) [27].

Recent studies provide quantitative evidence supporting the superior preservation of coagulation factors following PDI treatment. For example, after photoinactivation of plasma using riboflavin and UV light, the residual activity of key coagulation factors such as FVIII and fibrinogen (FI) remained at 61% and 69% of baseline values, respectively, even after effective bacterial inactivation [28]. These results are consistent with earlier findings by Hornsey et al. [29], who reported FVIII retention of 68.5% and fibrinogen retention of 78.8% following similar photochemical protocols. Importantly, these retention rates compare favorably to those observed with solvent/detergent (S/D) plasma, where in vitro studies have shown a mild reduction of 10%–20% in some coagulation factors and inhibitor activity.

Furthermore, photochemical treatments based on amotosalen and UVA light have been shown to preserve the majority of coagulation proteins within physiologic ranges, with mean recoveries for most factors between 81% and 97%, and only FVIII showing a more pronounced reduction to approximately 69% [30]. Collectively, these data underscore that PDI protocols, particularly those employing optimized photosensitizer concentrations and fractionated light dosing, can achieve robust pathogen reduction while maintaining clinically relevant levels of coagulation factor activity, an essential criterion for transfusion safety

and efficacy [15,31,32].

Our approach offers distinct advantages over existing pathogen reduction technologies. Unlike the INTERCEPT and Mirasol systems [30] which utilize UVA activation of synthetic photosensitizers, Photogem® leverages deeper-penetrating red light (630 nm) and leaves no synthetic residues with uncertain long-term effects. The modular, fractionated protocol developed here adapts to variable plasma volumes and oxygen diffusion limitations, addressing key barriers to clinical translation [30,33–36].

For biocompatibility, as with other blood pathogen inactivation platforms (e.g., INTERCEPT, Mirasol), clinical use of Photogem® mediated PDI would require strict verification that residual photosensitizer and its photoproducts in treated plasma remain below recognized safety thresholds prior to transfusion. Such safety testing and regulatory assessment are standard for all clinical pathogen inactivation modalities [30,36].

By resolving the critical trade off between pathogen inactivation and plasma preservation, this work provides a photochemical framework for enhancing transfusion safety in the era of antibiotic resistance. The developed parameters offer immediate utility for blood banks, while the mechanistic insights into plasma photosensitizer interactions inform next generation PDI strategies for biologics sterilization.

A key limitation of this study is the exclusive use of artificial plasma, which, while clinically relevant, does not fully replicate the complexity of human plasma. Future studies should validate these findings in real plasma to confirm the retention of coagulation function and optimize clinical translation.

5 Conclusion

Photodynamic inactivation (PDI) using Photogem® presents a transformative approach to plasma decontamination, addressing the critical challenge of bacterial contamination while preserving therapeutic functionality. This study demonstrates that PDI achieves clinically relevant reductions of *Staphylococcus aureus* in plasma through optimized protocols that leverage plasma's molecular complexity as an advantage rather than a limitation. The inherent protein composition of plasma stabilizes Photogem®, prolonging its activity and enabling sustained reactive oxygen species (ROS) generation while mitigating photobleaching, a key advancement over conventional methods that compromise plasma integrity.

The development of fractionated illumination protocols overcame oxygen diffusion barriers inherent to viscous media, enhancing bacterial inactivation efficacy. Crucially,

this approach meets FDA sterilization thresholds for blood products without degrading coagulation factors, positioning PDI as a viable alternative to UV-C and solvent detergent technologies.

These findings redefine plasma decontamination paradigms by resolving the longstanding trade-off between pathogen eradication and biomaterial preservation. Future translation requires scaling this photochemical strategy to clinical systems, with immediate applications in blood bank safety protocols. Expanding validation to viral and fungal pathogens, alongside integration into closed loop plasma storage devices, will further establish PDI as a versatile, resistance agnostic sterilization modality. By bridging photochemical innovation with transfusion medicine needs, this work advances toward safer blood products in an era of escalating antimicrobial resistance.

Together, these advances position Photogem®-mediated PDI as a practical, scalable, and clinically ready pathway to safer plasma, poised to elevate transfusion standards while preserving therapeutic function

Statements and Declarations

Ethics approval and consent to participate Not applicable. This study did not involve human participants or animals.

Competing interests The authors declare that they have no competing interests.

Acknowledgements This research was financially supported by Cancer Prevention and Research Institute of Texas (CPRIT, Grant RR220054), Governor's University Research Initiative (GURI), and Chancellor's Research Initiative (CRI). São Paulo Research Foundation (FAPESP, Grant 2024/00100-0, 2025/26084-6), National Council for Scientific and Technological Development (CNPq, Grant 400468/2024-6), and Brazilian Agency for Research and Industrial Innovation (Embrapii - Basic Funding in Oncology).

Data Availability The data sets used and/or analyzed will be available from the corresponding author upon reasonable request.

Author Contributions Conceptualization: A.T., J.M.S., V.V.Y.; Methodology: A.T., J.M.S., V.S.B.; Investigation: A.T.; Supervision: V.S.B.; Writing—original draft: A.T., J.M.S.; Writing—review editing: A.T., J.M.S., V.S.B.

Open Access This article is licensed under a Creative Commons Attribution 4.0 International License, which permits use, sharing, adaptation, distribution and reproduction in any medium or format, as long as you give appropriate credit to the original author(s) and the source, provide a link to the Creative Commons licence, and indicate if changes were made. The images or other third party material in this article are included in the article's Creative Commons licence, unless indicated otherwise in a credit line to the material. If material is not included in the article's Creative Commons licence and your intended use is not permitted by statutory regulation or exceeds the permitted use, you will need to obtain permission directly from the copyright holder. To view a copy of this licence, visit <http://creativecommons.org/licenses/by/4.0/>.

References

1. Delaney, J., Schneider-Lindner, V., Brassard, P., Suissa, S.: Mortality after infection with methicillin-resistant *Staphylococcus aureus* (MRSA) diagnosed in the community. *BMC Med* **6**(1), 2 (2008)
2. Seltam, A., Müller, T.H.: UVC irradiation for pathogen reduction of platelet concentrates and plasma. *Transfus. Med. Hemother* **38**(1), 43–54 (2011)
3. Hellstern, P., Solheim, B.G.: The use of solvent/detergent treatment in pathogen reduction of plasma. *Transfus. Med. Hemother* **38**(1), 65–70 (2011)
4. Stewart, C.F., Tomb, R.M., Ralston, H.J., Armstrong, J., Anderson, J.G., MacGregor, S.J., Atreya, C.D., Maclean, M.: Violet-blue 405-nm light-based photoinactivation for pathogen reduction of human plasma provides broad antibacterial efficacy without visible degradation of plasma proteins. *Photochem. Photobiol* **98**(2), 504–512 (2022)
5. Kwakman, J.A., Vos, M.C., Bruno, M.J., Thieme, G., Kg, V.: Investigation of the efficacy of an innovative endoscope drying and storage method in a simulated ERCP setting. *Endosc. Int. Open* **11**(4), E419–E425 (2023)
6. van Minnen, O., van den Bergh, W.M., Kneyber, M.C.J., Accord, R.E., Buys, D., Meier, S.: Fresh frozen plasma versus solvent detergent plasma for cardiopulmonary bypass priming in neonates and infants undergoing cardiac surgery: A retrospective cohort study. *J. Cardiothorac. Vasc. Anesth* **38**(5), 1144–1149 (2024)
7. Vatansever, F., de Melo, W.C.M.A., Avci, P., Vecchio, D., Sadasivam, M., Gupta, A., Chandran, R., Karimi, M., Parizotto, N.A., Yin, R., Tegos, G.P., Hamblin, M.R.: Antimicrobial strategies centered around reactive oxygen species – bactericidal antibiotics, photodynamic therapy, and beyond. *FEMS Microbiol. Rev* **37**(6), 955–989 (2013)
8. Machado Soares, J., Quatrini Corre, T., Patricia Barrera Patin, C., Salgado Gonc, I., Grube dos Santos, G., Gomes Guimara, G., Vieira de Lima, R., Hellen Nunes Lima, T., Carolina Corre, B., Cruz de Souza Cappellini, T., Vitória Silva Pereira, M., Oliveira Resende A.L.F., Yakovlev, V.V., Cristina Blanco, K., Salvador Bagnato, V.: Synergistic paradigms in infection control: A review on photodynamic therapy as an adjunctive strategy to antibiotics. *ACS Infect. Dis* **11**(10), 2671–2691 (2025)
9. Hamblin, M.R., Hasan, T.: Photodynamic therapy: a new antimicrobial approach to infectious disease? *Photochem. Photobiol. Sci* **3**(5), 436–450 (2004)
10. Wainwright, M., Maisch, T., Nonell, S., Plaetzer, K., Almeida, A., Tegos, G.P., Hamblin, M.R.: Photoantimicrobials—are we afraid of the light? *Lancet Infect. Dis* **17**(2), e49–e55 (2017)
11. Star, W.M.: Light delivery and light dosimetry for photodynamic therapy. *Lasers Med. Sci* **5**(2), 107–113 (1990)
12. Kim, M.M., Darafsheh, A.: Light sources and dosimetry techniques for photodynamic therapy. *Photochem. Photobiol* **96**(2), 280–294 (2020)
13. Piksa, M., Lian, C., Samuel, I.C., Pawlik, K.J., Samuel, I.D.W., Matczyszyn, K.: The role of the light source in antimicrobial photodynamic therapy. *Chem. Soc. Rev* **52**(5), 1697–1722 (2023)
14. Soares, J.M., Corrêa, T.Q., Inada, N.M., Bagnato, V.B., Blanco, K.C.: In vitro study of photodynamic therapy for treatment of bacteremia in whole blood. *J. Pharm. Pharmacol* **6**(9), 863–869 (2018)
15. Corrêa, T.Q., Blanco, K.C., Soares, J.M., Inada, N.M., Kurachi, C., Golim, M.D.A., Deffune, E., Bagnato, V.S.: Photodynamic inactivation for in vitro decontamination of *Staphylococcus aureus* in whole blood. *Photodiagn. Photodyn. Ther* **28**, 58–64 (2019)
16. Menezes, P.F.C., Bagnato, V.S., Johnke, R.M., Bonnerup, C., Sibata, C.H., Allison, R.R., Perussi, J.R.: Photodynamic therapy for Photogem® and Photofrin® using different light wavelengths in 375 human melanoma cells. *Laser Phys. Lett* **4**(7), 546–551 (2007)
17. Ferreira, J., Menezes, P.F.C., Kurachi, C., Sibata, C.H., Allison, R.R., Bagnato, V.S.: Comparative study of photodegradation of three hematoporphyrin derivative: Photofrin®, Photogem®, and Photosan®. *Laser Phys. Lett* **4**(10), 743–748 (2007)
18. Stranadko, E.P., Skobelkin, O., Litwin, G., Astrakhankina, T.A.: Clinical photodynamic therapy of malignant neoplasms. In: *Proceedings of 1994 International Symposium on Biomedical Optics Europe*. 2325, 240–246 (1995)
19. Bellnier, D.A., Greco, W.R., Loewen, G.M., Nava, H., Oseroff, A.B., Dougherty, T.J.: Clinical pharmacokinetics of the PDT photosensitizers porfimer sodium (photofrin), 2-[1-hexyloxyethyl]-2-devinyl pyropheophorbide-a (photochlor) and 5-ALA-induced protoporphyrin IX. *Lasers Surg. Med* **38**(5), 439–444 (2006)
20. Alves, F., Stringasci, M.D., Requena, M.B., Blanco, K.C., Dias, L.D., Corrêa, T.Q., Bagnato, V.S.: Randomized and controlled clinical studies on antibacterial photodynamic therapy: An overview. *Photonics* **9**(5), 340 (2022)
21. Kou, J., Dou, D., Yang, L.: Porphyrin photosensitizers in photodynamic therapy and its applications. *Oncotarget* **8**(46), 81591–81603 (2017)
22. Sobotta, L., Skupin-Mrugalska, P., Piskorz, J., Mielcarek, J.: Porphyrinoid photosensitizers mediated photodynamic inactivation against bacteria. *Eur. J. Med. Chem* **175**, 72–106 (2019)
23. Maisch, T., Eichner, A., Späth, A., Gollmer, A., König, B., Regensburger, J., Bäuml, W.: Fast and effective photodynamic inactivation of multiresistant bacteria by cationic riboflavin derivatives. *PLoS One* **9**(12), e111792 (2014)
24. Woodhams, J.H., MacRobert, A.J., Bown, S.G.: The role of oxygen monitoring during photodynamic therapy and its potential for treatment dosimetry. *Photochem. Photobiol. Sci* **6**(12), 1246–1256 (2007)
25. Maisch, T., Baier, J., Franz, B., Maier, M., Landthaler, M., Szeimies, R.M., Bäuml, W.: The role of singlet oxygen and oxygen concentration in photodynamic inactivation of bacteria. *Proc. Natl. Acad. Sci. U.S.A* **104**(17), 7223–7228 (2007)
26. Lambrechts, S.A.G., Aalders, M.C.G., Verbraak, F.D., Lagerberg, J.W.M., Dankert, J.B., Schuitmaker, J.J.: Effect of albumin on the photodynamic inactivation of microorganisms by a cationic porphyrin. *J. Photochem. Photobiol. B* **79**(1), 51–57 (2005)
27. Schulze, T.J., Gravemann, U., Seltam, A.: THERAFLEX ultraviolet C (UVC)-based pathogen reduction technology for bacterial inactivation in blood components: Advantages and limitations. *Ann. Blood* **7**, 28 (2022)
28. Larrea, L., Calabuig, M., Roldán, V., Rivera, J., Tsai, H.M., Vicente, V., Roig, R.: The influence of riboflavin photochemistry on plasma coagulation factors. *Transfusion and Apheresis Science* **41**(3), 199–204 (2009)
29. Hornsey, V.S., Drummond, O., Morrison, A., McMillan, L., MacGregor, I.R., Prowse, C.V.: Pathogen reduction of fresh plasma using riboflavin and ultraviolet light: Effects on plasma coagulation proteins. *Transfusion* **49**(10), 2167–2172 (2009)
30. Schlenke, P., Hergig, T., Isola, H., Wiesel, M.L., Kientz, D.,



- Pinkoski, L., Singh, Y., Lin, L., Corash, L., Cazenave, J.P.: Photochemical treatment of plasma with amotosalen and UVA light: process validation in three European blood centers. *Transfusion* **48**(4), 697–705 (2008)
31. Crocker, L.B., Lee, J.H., Mital, S., Mills, G.C., Schack, S., Bistrovic-Popov, A., Franck, C.O., Mela, I., Kaminski, C.F., Christie, G., Fruk, L.: Tuning riboflavin derivatives for photodynamic inactivation of pathogens. *Scientific Reports* **12**, 6580 (2022)
 32. Xu, F., Feyissa, Q., Ibrahim, Z., Li, Y., Xu, K.L., Guo, Z., Ahmad, J., Vostal, J.G.: Inactivation of bacteria in plasma by photosensitizers benzophenone and vitamins K3, B1 and B6 with UV A light irradiation. *Photodiagn. Photodyn. Ther* **30**, 101713 (2020)
 33. Wasiluk, T., Rogowska, A., Boczkowska-Radziwon, B., Zebrowska, A., Bolkun, L., Piszcz, J., Radziwon, P.: Maintaining plasma quality and safety in the state of ongoing epidemic – The role of pathogen reduction. *Transfus. Apheresis Sci* **60**(1), 102953 (2021)
 34. Douplik, A.Y., Strattonnikov, A.A., Loschenov, V.B., Lebedeva, V.S., Derkacheva, V.M., Vitkin, I.A., Romyanceva, V.D., Kusmin, S.G., Mironov, A.F., Lukyanets, E.A.: Study of photodynamic reactions in human blood. *J. Biomedical Optics* **5**(3), 338–349 (2000)
 35. Wainwright, M.: Methylene blue derivatives — suitable photoantimicrobials for blood product disinfection? *Int. J. Antimicrob. Agents* **16**(4), 381–394 (2000)
 36. Maccaferri, C., Gherardi, M., Laurita, R.: Evaluating atmospheric pressure cold plasma decontamination techniques for packaging materials: a systematic review and meta-analysis. *Front. Phys. (Lausanne)* **12**, 1399720 (2024)



Anany Tewari is a Biomedical Engineering graduate specializing in medical device design, development, and regulatory compliance. She has research experience as a Graduate Research Assistant, where she contributed to projects in photodynamic therapy for infection treatment, focusing on protocol optimization and regulatory standards. Anany is proficient and interested in advancing healthcare technology through product development and quality assurance.

Anany Tewari is a Biomedical Engineering graduate specializing in medical device design, development, and regulatory compliance. She has research experience as a Graduate Research Assistant, where she contributed to projects in photodynamic therapy for infection treatment, focusing on protocol optimization and regulatory standards. Anany is proficient and interested in advancing healthcare technology through product development and quality assurance.



Jennifer M. Soares is a postdoctoral researcher in Biomedical Engineering at Texas A&M University. She holds a Ph.D. in Biomolecular Physics from the University of São Paulo. With a background in applied physics and biomolecular sciences, her research focuses on biophotonics, with an emphasis on developing and optimizing PDT for infection control and studying resistance mechanisms in clinically relevant bacteria.

Dr. Soares is an expert in advanced analytical methods such as FTIR spectroscopy and metabolic tests, and has helped to design procedures for efficient light-based therapy. She has published in peer-reviewed publications, won a gold prize in the International Genetically Engineered Machine (iGEM) competition, and garnered other academic accolades. Dr. Soares is dedicated to bridging fundamental research with clinical application, finding solutions to multidrug-resistant illnesses through interdisciplinary collaboration.



Vanderlei S. Bagnato is a Professor of Biomedical Engineering at Texas A&M and the University of São Paulo (USP), and a distinguished member of both the National Academy of Engineering (International) and the National Academy of Sciences (International). He holds B.S. degrees in Physics from IFSC-USP and in Materials Science and Engineering from the Federal University of São Carlos, and completed a Ph.D. in

Physics from the Massachusetts Institute of Technology. Professor Bagnato is internationally recognized for his pioneering research in atomic and molecular physics, which includes studies of quantum turbulence in atomic superfluids, laser cooling and trapping of neutral atoms, and work in time and frequency metrology, which is exemplified by the creation of the first atomic clock and high-precision microscope pilot plant in Latin America. His work also focuses on the use of lasers and optics in health sciences, particularly the clinical use of photodynamic therapy for microbiological control and cancer treatment in Brazil. He has actively collaborated with academic institutions worldwide and promoted science through public exhibitions and specialist TV channels, as part of his commitment to scientific dissemination.